

Cholesterol Dynamics in Membranes of Raft Composition: A Molecular Point of View from ^2H and ^{31}P Solid-State NMR

Fabien Aussenac, Marianne Tavares, and Erick J. Dufourc*

Institut Européen de Chimie et Biologie, Ecole Polytechnique, CNRS & Universités de Bordeaux I et II, Pessac, France

Received August 23, 2002; Revised Manuscript Received November 18, 2002

ABSTRACT: Lipidic membrane systems that have been reported to be composed of sphingomyelin (SM)-cholesterol (Chol) microdomains or “rafts” by Dietrich et al. [palmitoyl-oleoyl-phosphatidylcholine(POPC)/SM/Chol, 1/1/1; Dietrich, C., Bagatolli, L. A., Volovyk, Z. N., Thompson, N. L., Levi, M., Jacobson, K., and Gratton, E. (2001) *Biophys. J.* 80, 1417–1428] and by Schroeder et al. [SCRL: Liver-PC/Liver-phosphatidylethanolamine/SM/Cerebrosides/Chol, 1/1/1/1/2; Schroeder, R., London, E., and Brown, D. (1994) *Proc. Natl. Acad. Sci. U.S.A.* 91, 12130–12134] were investigated under the form of fully hydrated liposomes by the noninvasive solid-state ^{31}P and ^2H NMR method. Liposomes of binary lipid composition POPC/Chol and SM/Chol were also studied as boundary/control systems. All systems are found to be in the liquid-ordered phase (Lo) at physiological temperatures. Use of deuterium-labeled cholesterol afforded finding both the position of the sterol motional axis and its molecular order parameter. The axis of anisotropic rotation of cholesterol is such that the molecule is, on average, quasiperpendicular to the membrane plane, in all of the four systems investigated. Cholesterol order parameters greater than 0.8 are observed, indicating that the sterol is in a very motionally restricted environment in the temperature range 0–60 °C. The binary mixtures present “boundary” situations with the lowest values for POPC/Chol and the highest for SM/Chol. The SCRL raft mixture has the same ordering as the SM/Chol, i.e., the highest order parameter values over the temperature range. It demonstrates that in the SCRL mixture cholesterol dynamics is as in the binary system SM/Chol, therefore, suggesting that it might be depleted from the rest of the membrane to form complexes as if it were alone with SM. On the other hand, the mixture POPC/SM/Chol exhibits an intermediate ordering situation between those of SM/Chol and POPC/Chol. This strongly suggests that cholesterol could be in fast exchange, at the NMR time scale (milli- to microseconds), between two or more membrane regions of different dynamics and questions the statement of “rigid domains” made of SM and cholesterol in the model “raft” system POPC/SM/Chol.

A new concept is emerging in biology in relation with the lateral organization of biomembranes: it is proposed that lipid microdomains, also denominated rafts, exist in the plane of the membrane and could explain some complex biological activity. These lipid microdomains are rich in cholesterol and sphingomyelin and could be stabilized by weak forces such as hydrogen bonding and van der Waals interactions between glycosphingolipids. The rafts also possess distinct protein composition, favoring development of signal transduction or membrane trafficking because of the formation of confined regions (1–4). Several physicochemical methods reported domains observation in membrane models containing cholesterol, including fluorescence (5–7) and atomic force microscopy (AFM)¹ (8). These studies described domains existence on supported mono- and bilayers, giant unilamellar vesicles (GUV) made of gangliosides, sphingomyelin (SM), phospholipids (dipalmitoylphosphatidylcholine, DPPC; dipalmitoylphosphatidyl-ethanolamine, DPPE; dioleoylphosphatidylethanolamine, DOPE; ...) and cholesterol

(Chol). In the above works, the microdomain’s size was estimated to range from 10 to 70 μm . However, in biomembranes, there are a variety of factors (e.g., proteins) that limit the size of rafts to considerably smaller dimensions than those reported in model membranes. Moreover, in some cases, the spectroscopic techniques implied invasive or nonnatural probes (lipid analogues with a fluorescent probe) or solid supported media to reproduce the membrane. The fluorescent probes, such as rhodamine and Laurdan, may perturb the system by favoring the formation or aggregation of lipid microdomains by intrinsic cross-linking of the probes that are used for the detection. A general concept, which subtends all the above studies, is the rafts rigidity, which would be due to the presence of increased concentrations of cholesterol and sphingomyelin. This very rigid character, as opposed to

* To whom correspondence should be addressed. Telephone/Fax: (33) +5 57 96 22 18. E-mail: erick.dufourc@iecb-polytechnique.u-bordeaux.fr.

¹ Abbreviations: AFM, atomic force microscopy; Chol, cholesterol; Chol- $^2\text{H}_5$, deuterated cholesterol; CSA, chemical shift anisotropy; DMPC, dimyristoylphosphatidylcholine; DOPE, dioleoylphosphatidylethanolamine; DPPC, dipalmitoylphosphatidylcholine; DPPE, dipalmitoylphosphatidyl-ethanolamine; GUV, giant unilamellar vesicles; Lo, liquid-ordered phase; MLV, multilamellar vesicles; NMR, nuclear magnetic resonance; POPC, palmitoyl-oleoylphosphatidylcholine; SCRL, sphingomyelin cholesterol rich liposomes; SM, sphingomyelin.

the rest of the membrane in which rafts diffuse, would play an important role in the functional properties of proteins that are there embedded. However, to our knowledge, this rigidity has never been directly measured, at least using a noninvasive method.

The rigidity of a membrane is difficult to define. When using a macromolecular technique to probe membrane dynamics, one could state that it is the inverse of fluidity. But all molecular techniques, such as spectroscopies, probe at the atomic or molecular level. Hence the concept of molecular order parameter is best used to define the residual ordering of molecules in a membrane phase. A membrane that is made of molecules that have a very low order parameter (near the minimum value of 0) has little internal cohesion: it is almost as a liquid. At contrary, a membranous molecule that has an elevated molecular order parameter (near the maximum value of 1) is almost perfectly oriented with the director of motion (usually the bilayer normal). In this context the role of cholesterol on lipid membranes has been well-characterized, using a wide variety of techniques. Increasing concentrations of cholesterol in the membrane increases the membrane ordering. For instance, 30 mol % cholesterol in DMPC has been shown to lead to an order parameter (as reported by the phospholipid or the cholesterol) near 1, at ambient temperatures (9–11). In these conditions, the membrane reaches its maximum thickness. There is indeed a direct relationship between the increase in membrane ordering (decrease in lipid gauche defects in the bilayer core) and the increase in bilayer thickness (12, 13). The physical state of this cholesterol-rich membrane is called “liquid-ordered” (L_o) because it shares properties of fluid- L_α and gel- L_β phases (14–16).

We describe herein a noninvasive approach to characterize the rafts molecular ordering: solid-state NMR spectroscopy. NMR spectra are a well-known means for distinguishing different lipid phases at the microsecond time scale (17–20). This has been recently illustrated by the work of Franzin and Macdonald (21) on mixtures of cationic polyelectrolytes and anionic phospholipids. These authors observe domains that are characterized by distinct quadrupolar splitting on deuterium spectra. The order parameter, which is directly measured from spectra, affords a precise measurement of membrane “microfluidity”. The bilayer thickness that is linked to membrane elasticity can be also calculated from such data (12, 22, 23). Different dynamical behaviors, at the nanosecond time scale, may also be obtained from nuclear relaxation experiments. This strategy is developed herein for the first molecular description of raft model membranes. We used synthetic deuterium-labeled cholesterol (Chol- 2H_5) as a probe for dynamics of rafts model membrane systems. The isotope of hydrogen, deuterium, can really be considered as noninvasive reporter, and 2H NMR has already been used to accurately describe the molecular structure and dynamics of cholesterol in model membranes (10, 11, 24). We choose to work on the same rafts model membranes as in the works of Dietrich et al. (7) (POPC/SM/Chol-d5, 1/1/1) and Schroeder et al. (25) (SCRL: Liver-phosphatidylcholine/Liver-phosphatidylethanolamine/SM/Cerebrosides/Chol-d5, 1/1/1/1/2). These rafts mixtures were reported to be characteristic of microdomains as observed by fluorescence and ultracentrifugation techniques, respectively.

The structural and dynamical properties of cholesterol in the rafts model membranes were determined by calculation of its molecular order parameter, S_{mol} , and the location of the principal axis of motion (axis of inertia) within the steroid structure. Nuclear relaxation times T_{1Z} and T_{2E} were also measured. Deuterium NMR spectra simulations were also realized, on the basis of experimental spectra, to evaluate the possible domains observation by solid-state NMR.

EXPERIMENTAL PROCEDURES

Chemicals. Brain sphingomyelin (SM), 1-palmitoyl-2-oleoyl-*sn*-3-phosphocholine (POPC), liver phosphatidylcholine (Liver-PC), liver phosphatidylethanolamine (Liver-PE), and brain cerebrosides were purchased from Avanti Polar Lipids (Birmingham, AL) and used without further purification. Cholesterol deuterated at the 2,2,4,4,6 positions (Chol- 2H_5) was synthesized according to the procedure described by Dufourc et al. (10). Deuterium-depleted water was obtained from Eurisotop (Saint Aubin, France).

Sample Preparation. Appropriate amounts of phospholipids and labeled cholesterol (10 mg Chol- 2H_5 , 33% by mol) were dissolved in a chloroform-methanol mixture (90/10 v/v). Organic solvents were evaporated and the resulting lipid film was dried under high vacuum pumping during several hours. To remove residual solvent, three successive freeze-drying steps were realized with a large excess of deuterium-depleted water. Dispersions of phospholipids were prepared in deuterium-depleted water to reach about 90% hydration (w/w). Finally, three freeze-thaw cycles, with shaking in a vortex mixer, were repeated to achieve a better homogeneity in liposomes formation. The resulting multilamellar dispersion was transferred into a 7 mm NMR tube (300 μ L) for wide line NMR experiments.

NMR Spectroscopy. NMR experiments were carried out on a Bruker Avance DSX 500 machine (11.75 T). ^{31}P NMR spectra were acquired at 202.46 MHz using a phase-cycled Hahn-echo pulse sequence with gated broadband proton decoupling (26). Deuterium NMR experiments on labeled cholesterol were performed at 76.77 MHz by means of the quadrupolar echo pulse sequence $90^\circ x - \tau - 90^\circ y - \tau - \text{acq}$ (27). Typical acquisition parameters were as follows: spectral window of 50 kHz for ^{31}P NMR and 500 kHz for 2H NMR; $\tau/2$ pulse widths ranged from 3 to 5 μ s depending on sample, interpulse delays, τ , were of 30–40 μ s. A recycle delay of 5 s was used for ^{31}P NMR; for 2H NMR experiments, it was set to 100 ms (i.e., more than 10 times the longest T_{1Z}). Typically, 128K acquisitions were recorded for deuterium nucleus and 512 transients for phosphorus nucleus. Quadrature detection was used in all cases. Samples were allowed to equilibrate at least 30 min at a given temperature (ranging from 0 to 60 $^\circ$ C) before the NMR signal was acquired; the temperature was regulated to ± 1 $^\circ$ C.

Deuterium T_{1Z} relaxation times were recorded by the inversion quadrupolar echo sequence $180^\circ - t_1 - 90^\circ x - \tau - 90^\circ y - \tau - \text{acq}$. The delay t_1 was varied from 3 μ s to 100 ms. At least 25 t_1 values were used to characterize the inversion-recovery decay curves. The recovery of the magnetization after a 180° pulse followed a single exponential for each assigned quadrupolar splitting. The decay of the area under a particular assigned spectral component (90° orientation of the Pake doublet) was fitted as a function of t_1 values to an exponential

law: $M_Z(t_1)/M_0 = 1 - A \exp(-t_1/T_{1Z})$ where the coefficients A and T_{1Z} were adjustable (the coefficient A was very close to 2). Transverse relaxation times, T_{2E} , were evaluated using the standard quadrupolar echo pulse sequence: $90^\circ_x - t_2 - 90^\circ_y - \tau - \text{acq}$, and the t_2 delay was varied between 30 and 400 μs . The quadrupolar echo decay was fitted according to the equation $M_{xy}(t_2)/M_0 = B \exp(-2t_2/T_{2E})$, and T_{2E} values were extracted for each spectral component. The B coefficient was found very close to 1.

Calculations. Spectral second moments (M_2) were calculated with a FORTRAN routine according to Davis (17) and used to determine the phase transition temperature, T_c , in the different liposome compositions. Oriented ^2H NMR spectra at 90° were obtained by the numerical de-Pake-ing routine (28, 29). A FORTRAN program (E.J.D., unpublished material) was used to transform the atomic coordinates of cholesterol into the axis system C (see Appendix and Figure 6 for definition of axis system). It was also used to calculate the principal axis of motion \vec{n} of the cholesterol molecule and its molecular order parameter S_{mol} (see Appendix). Data fitting for NMR relaxation experiments was accomplished with the Origin software (OriginLab Corp. Northampton, MA). All the representations of cholesterol molecule were visualized on WebLabViewerLite 3.2 and on InsightII (Molecular Simulations, Inc.). Analyses of C–D bond orientation relative to the principal axis of motion \vec{n} were performed within the Decipher module of the Insight package. Deuterium NMR spectra simulations were realized using a FORTRAN program (Dufourc, unpublished).

Theoretical Background. In biomembranes, the phospholipids exist in a liquid crystalline state and the structural properties of these molecules can therefore be described in terms of order parameters. When the motions of the C–D segments are axially symmetric, one can relate the residual quadrupolar splittings, $\Delta\nu_Q$, of the ^2H NMR spectrum to the orientational order parameter, S_i^{CD} , of the i th C–D bond vector according to (17, 30):

$$\Delta\nu_Q^i(\theta') = \frac{3}{2} A_Q \frac{3 \cos^2 \theta' - 1}{2} S_i^{\text{CD}} \quad (1)$$

The static deuterium quadrupolar coupling constant A_Q ($A_Q = e^2 q Q / h$) is 167 kHz for aliphatic C–D bonds (31). The angle θ' is that between the bilayer normal and the magnetic field. In the particular case of a rigid molecule such as the fused ring system of cholesterol, where conformational disorder is negligible, the expression of S_i^{CD} depends on the orientation of the C_{*i*}–D bond, angle γ_i , with respect to the principal axis of motion of the molecule, \vec{n} , and the so-called molecular order parameter, S_{mol} , accounting for the “wobbling-in-a-cone” anisotropic diffusion of cholesterol (9, 32). Such a parameter varies between 1, when there are no molecular oscillations with respect to \vec{n} , and 0, when all orientations are allowed as in a liquid phase. As an example, a value of 0.8 leads to a semi-angle for oscillations in a cone of about 13° (9). Hence, the observable S_i^{CD} is directly proportional to S_{mol} (10, 11, 24):

$$S_i^{\text{CD}} = S_{\text{mol}} \left(\frac{3 \cos^2 \gamma_i - 1}{2} \right) \quad (2)$$

The molecular order parameter is the same for all C–D

bonds linked to the rigid structure. However, these bonds can give rise to different S_i^{CD} values depending upon their geometrical orientations $[(3 \cos^2 \gamma_i - 1)/2]$ with respect to the axis of motion. A general method for evaluating separately S_{mol} and $[(3 \cos^2 \gamma_i - 1)/2]$ in eq 2 has been already proposed (10, 11, 24). This approach is based on the calculation of the position of the axis of motion \vec{n} in the rigid structure. The orientation of \vec{n} is defined by two angles α and β in a molecular frame attached to the molecule. In the procedure, the angles α and β are varied until the calculated and the experimental terms $P_2(\cos \gamma_i)$ match. Once the orientation of \vec{n} has been correctly determined, $P_2(\cos \gamma_i)$ is known for a given C–D bond, the molecular order parameter, S_{mol} , can be directly obtained from eq 2.

RESULTS

NMR experiments were realized on two lipids/labeled cholesterol “rafts” compositions: POPC/SM/Chol- $^2\text{H}_5$ (1/1/1, molar fractions) and Liver-PC/Liver-PE/SM/Cerebrosides/Chol- $^2\text{H}_5$ (1/1/1/1/2, SCRL composition). Two binary compositions, POPC/Chol- $^2\text{H}_5$ (2/1) and SM/Chol- $^2\text{H}_5$ (2/1), were also investigated to achieve comprehensive analysis. Wide line deuterium and phosphorus NMR experiments were performed on these four model membrane mixtures over a wide range of temperatures (from 0 to 60 $^\circ\text{C}$). We also measured T_{1Z} and T_{2E} relaxation times of labeled cholesterol positions to probe dynamics at the nanosecond time scale.

^2H NMR Spectroscopy of Labeled Cholesterol. Figure 1 shows ^2H NMR cholesterol spectra for the four mixtures at three characteristic temperatures (5, 20, and 30 $^\circ\text{C}$). Acquisition conditions were kept identical for all spectra (same number of scans and same recycle delay). In the case of the binary system POPC/Chol- $^2\text{H}_5$ (2/1), we observe the typical axially symmetric powder pattern line shape that reflects the fast axially symmetric reorientation of deuterated cholesterol whatever the temperature recorded (0–60 $^\circ\text{C}$). Three distinct quadrupolar splitting are easily assigned in reference to previous work on model membranes composed of DMPC/Chol- $^2\text{H}_5$ (2/1) (10): a small one, indicating that this position (cholesterol carbon 6) is almost at the magic angle (54.7°), the second intermediate quadrupolar splitting corresponding to the equatorial conformations of the 2,4 labeled positions and the largest one assigned to the axial conformations of the 2,4 labeled positions. Deuterium NMR spectra of the second binary system, SM/Chol- $^2\text{H}_5$ (2/1), present a different behavior as a function of temperature. At low temperature, i.e., 5 $^\circ\text{C}$, almost no signal is detected: cholesterol is apparently immobilized in the membrane and leads to a very broad component [theoretical $\Delta\nu_Q(90^\circ)$ close to 125 kHz] that is barely detectable under the present acquisition conditions (spin–spin relaxation time very short). The weak residual isotropic line is assigned to residual deuterated water (HOD) or to a little amount of small vesicles that tumble rapidly. When the temperature is increased to 20 and 30 $^\circ\text{C}$, the motions of the cholesterol moiety, such as rapid reorientation, become active and lead to a reduction of the quadrupolar splitting (partial averaging of the static quadrupolar interaction) and to an increase of the spin–spin relaxation time therefore leading to signal detection. Concerning the two rafts mixtures (POPC/SM/Chol- $^2\text{H}_5$ and SCRL), cholesterol is not immobilized at 5 $^\circ\text{C}$, but one detects an intermediate situation reflecting the incoming of cholest-

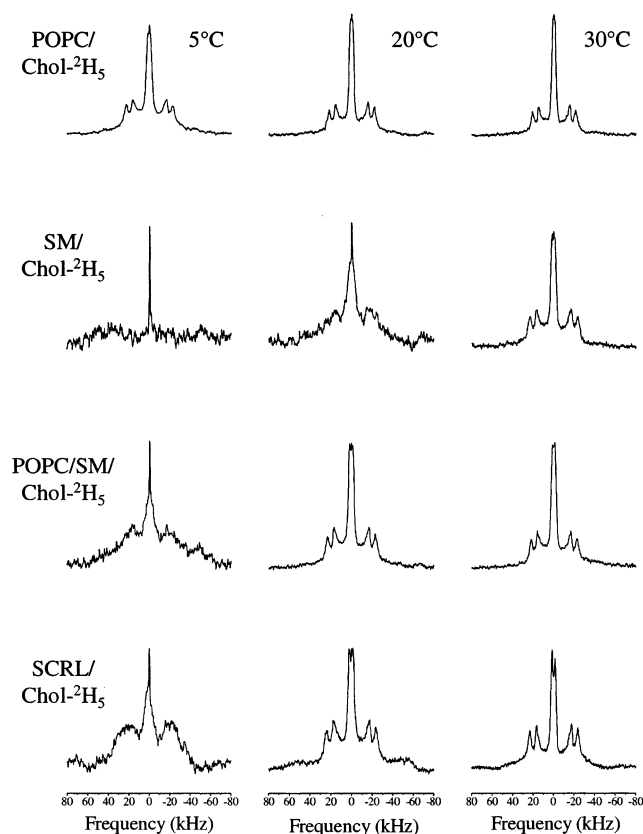


FIGURE 1: Deuterium NMR spectra of labeled cholesterol (Chol- $^2\text{H}_5$) in the four lipid-cholesterol mixtures: POPC/Chol- $^2\text{H}_5$, Sphingomyelin (SM)/Chol- $^2\text{H}_5$, and in the two "rafts" compositions POPC/SM/Chol- $^2\text{H}_5$, Sphingomyelin-Cholesterol-Rich Liposome (SCRL). Each composition contains 33 mol % of deuterium-labeled cholesterol. Only three representative temperatures are shown. Acquisition conditions were kept the same for all spectra: 90° pulse width, $3.5 \mu\text{s}$; interpulse delay, $30 \mu\text{s}$; recycle delay, 100 ms; 128K scans.

terol axial rotation. At 20°C and higher, spectra exhibit the well-known axially symmetric pattern characteristic of fast axial reorientation of cholesterol in model membranes (10, 24).

Figure 2 reports an expansion of ^2H NMR spectral line shape for all of the different lipids/cholesterol systems investigated, at 30°C . The vertical lines indicate the quadrupolar splitting of the 2,4 axial and equatorial positions for the two reference binary systems. The system POPC/Chol- $^2\text{H}_5$ presents the smallest $\Delta\nu_Q(90^\circ)$ (30.5 and 42.6 kHz, solid lines) whereas SM/Chol- $^2\text{H}_5$ has the largest (33.4 and 46.9 kHz, dashed lines). The POPC/SM/Chol- $^2\text{H}_5$ mixtures have intermediate $\Delta\nu_Q(90^\circ)$ values ranging between the previous binary systems; whereas the SCRL raft composition presents the same $\Delta\nu_Q(90^\circ)$ as those of the SM/Chol- $^2\text{H}_5$ binary system.

Spin-lattice relaxation times T_{1Z} and transverse relaxation T_{2E} were measured for all labeled cholesterol positions in the two rafts mixtures (POPC/SM/Chol- $^2\text{H}_5$ and SCRL). It is noteworthy that spectra kept the same global line shape during the relaxation experiments (no detectable spectral distortion). As already indicated, all intensity variations were monoexponential and could be well fit with equations written in the Experimental Procedures. At 30°C , the T_{1Z} values are 6.5 ms for the 6 position, 8.0 ms for the 2,4 axial position and 8.7 ms for the 2,4 equatorial position (10% of accuracy).

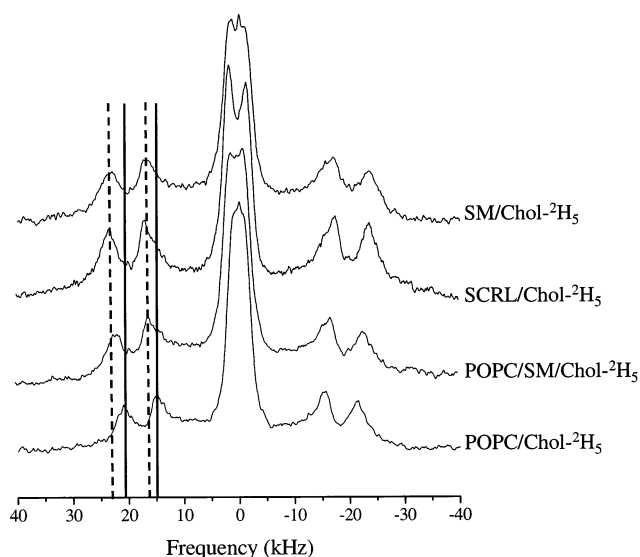


FIGURE 2: Expansion of deuterium NMR spectra of Chol- $^2\text{H}_5$ in the four lipid mixtures at 30°C . Solid lines are eye-guides to show the quadrupolar splittings of POPC/Chol- $^2\text{H}_5$ whereas dashed lines delineate those of SM/Chol- $^2\text{H}_5$.

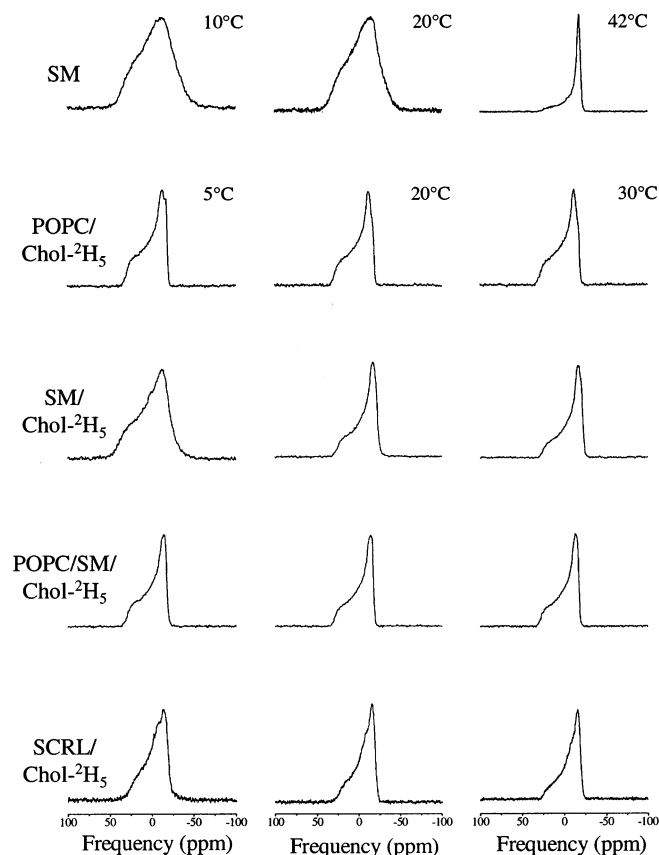


FIGURE 3: Proton-decoupled phosphorus NMR spectra for the four lipid-cholesterol compositions (same compositions as in Figure 1) and SM liposomes. Only representative temperatures are shown. Acquisition conditions are 90° pulse width, $5 \mu\text{s}$; interpulse delay, $30 \mu\text{s}$; recycle delay, 5 s; 512 scans.

The T_{2E} values are very short: 230 and $320 \mu\text{s}$ for positions 2,4 axial/equatorial and for the 6 position, respectively.

^{31}P NMR Spectroscopy. Figure 3 presents proton decoupled ^{31}P NMR spectra of the four lipids-cholesterol mixtures at three different characteristics temperatures (5°C , 20°C , and 30°C), and also spectra of pure SM liposomes. In all cases

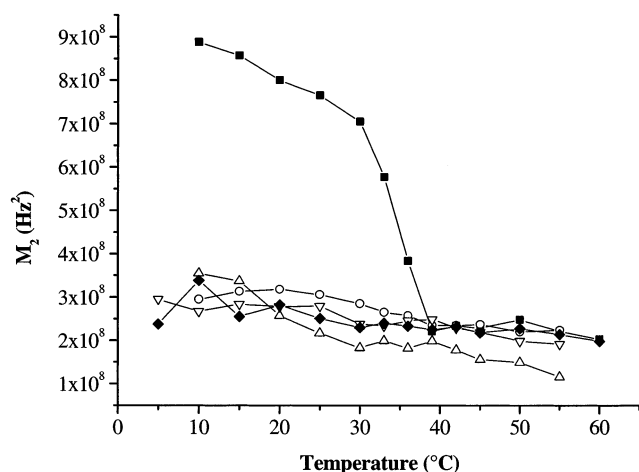


FIGURE 4: Thermal variation of spectral second moment, M_2 , of the four lipid-cholesterol compositions and of sphingomyelin liposomes. M_2 s were calculated from ^{31}P NMR spectra. (■) SM, (○) POPC/Chol- $^2\text{H}_5$, (△) SM/Chol- $^2\text{H}_5$, (▽) POPC/SM/Chol- $^2\text{H}_5$, (◆) SCRL/Chol- $^2\text{H}_5$. Accuracy is 1–5%.

(compositions and temperatures), spectra are characteristic of nonoriented multilamellar vesicles (MLV). Because of the rapid rotation of the lipids around an axis collinear to the normal to the bilayer, the phosphorus chemical shift anisotropy interaction (CSA) is partially averaged and leads to an axially symmetric powder pattern. Although there may be different CSA for each of the phospholipids in the mixtures, they cannot be clearly distinguished on spectra: an overall powder pattern is detected instead. Spectra of SM vesicles exhibit the usual behavior of lipid water dispersions undergoing a phase transition: a broad powder pattern is detected for temperatures in the $L_{\beta'}$ gel phase (10 and 20 °C) and for temperatures in the L_{α} fluid phase (42 °C, Figure 3) spectra exhibit the shape characteristic of fast uniaxial reorientation (33).

We calculated the second spectral moment, M_2 , for the temperature series (Figure 4). In all cholesterol-containing mixtures, we observe a monotonic M_2 variation of as a function of temperature (Figure 4). For SM liposomes, the second moment profile depicts the first-order phase transition between the $L_{\beta'}$ gel phase and the L_{α} fluid phase. A transition temperature, T_c , is detected at 35 °C, which is specific of the SM extract used. It is noteworthy that T_c was already reported to be 37 or 43 °C depending on the natural chain composition (34).

DISCUSSION

The use of solid-state NMR on four lipid mixtures, among which two are of so-called “raft” composition, brought the following results: (i) the gel-to-fluid phase transition is no longer detected on all the mixtures. (ii) The cholesterol spectrum in SM/Chol- $^2\text{H}_5$ is wider than in POPC/Chol- $^2\text{H}_5$, reflecting a more rigid behavior for the sterol in sphingomyelin membranes. (iii) The cholesterol spectrum in SCRL mixtures is identical, within the experimental error, to that of SM/Cholesterol mixtures, indicating a similar dynamical behavior for the sterol in both mixtures. (iv) The cholesterol spectrum in POPC/SM/Chol- $^2\text{H}_5$ mixture has a width that is halfway those observed for POPC/Chol- $^2\text{H}_5$ and SM/Chol- $^2\text{H}_5$ mixtures, on the temperature range of 20 to 60 °C. All these results will be discussed and quantified below by

calculation of cholesterol spectra, location of the axis of motional averaging, and molecular order parameter.

Thermotropism. Phosphorus NMR in biomembranes is affected both by the conformation of the phosphate group and by the polymorphism of lipids, i.e., the lipid phases. In our study it allowed to follow changes in the gel-to-fluid phase transition, T_c , of lipid mixtures. In the presence of cholesterol, phosphorus spectra retain the same shape and width over large temperature ranges (Figure 3). This is an indication of phase transition abolition (Figure 4) for all investigated systems. In model membranes made of one synthetic lipid plus cholesterol this behavior has been attributed to the appearance of a liquid-ordered phase (L_o) for cholesterol contents greater than 22% (16). The same phenomenon seems to occur here for the both rafts mixtures investigated as well as for the binary systems POPC/Chol and SM/Chol. It is worthwhile mentioning that recent work on bovine brain SM-cholesterol mixtures also concluded to phase transition abolition and to the appearance of a L_o phase (35).

Cholesterol Dynamics in Binary Systems. Although abolishing in the same way the phase transition of POPC and SM water dispersions, cholesterol presents different dynamics in these membranes. At low temperatures (5 °C), the signal of labeled cholesterol is no longer detectable in SM membranes. This indicates that its dynamics is considerably reduced and suggests that it may be immobilized in the membrane as it has been shown in similar binary systems when cholesterol is added in excess. Wassall and co-workers indeed reported a solid phase of cholesterol (with a $\Delta\nu_Q(90^\circ)$ of 118 kHz) for a system made of a (1/1) molar ratio of sterol and unsaturated phosphatidylcholine (36). This phase was in equilibrium with cholesterol rapidly reorienting in the membrane phase. In contrary, cholesterol shows its fast anisotropic reorientation in the POPC membrane at the same low temperature. Around 30 °C, cholesterol dynamics is similar in both POPC and SM systems: fast axial reorientation produces the well-known axially symmetric powder pattern as reported in DMPC and egg phosphatidylcholine (10, 24). However, close inspection at quadrupolar splitting indicates that cholesterol spectrum is wider in SM than in POPC.

The molecular order parameter can be calculated by the method described in the Appendix (vide infra, and Figure 7). It varies from 1 to 0.92 on going from 20 to 60 °C in the SM membranes. In the same temperature interval, it decreases from 0.93 to 0.81 in POPC dispersions. This indicates that the POPC/Chol membrane is much more dynamical than the SM/Chol system. The order parameter quantifies the wobbling of the cholesterol moiety. This demonstrates that at 30 °C, there is almost no wobbling in the SM membrane. The sterol is just spinning around its main symmetry axis. In contrary, in the case of POPC, the semi-angle of the cone of wobbling can be estimated according to Peterson and Chan (32) to ca. 13° at 30 °C. In other words, the SM/Chol membrane is a compact and rigid membrane whereas the POPC/Chol membrane is more disordered though its S_{mol} is markedly larger on comparing to that of a membrane in the absence of cholesterol ($S_{\text{mol}} = 0.7$ – 0.6 at 30 °C) (33).

Cholesterol Dynamics in Lipid “Domains”. Deuterium NMR spectra of both raft mixtures (Figure 2) have similar line shape than those of DMPC liposomes containing 33 mol

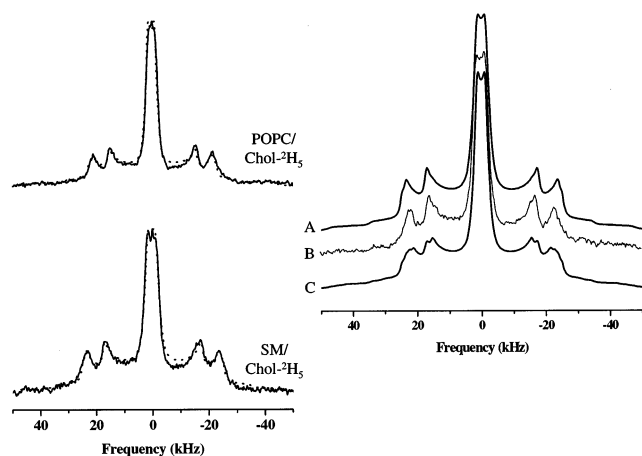


FIGURE 5: (Left) Simulated (superimposed dashed line) and experimental (solid line) deuterium-NMR spectra of POPC/Chol- $^2\text{H}_5$ and SM/Chol- $^2\text{H}_5$ at 30 °C. See text for details. (Right) Simulated (A, C) and experimental (B) spectra of the POPC/SM/Chol- $^2\text{H}_5$ system. Spectra A and C were obtained by a weighted addition of simulated POPC/Chol- $^2\text{H}_5$ and SM/Chol- $^2\text{H}_5$ spectra. (A) 0.9 SM/Chol- $^2\text{H}_5$ plus 0.1 POPC/Chol- $^2\text{H}_5$ and (C) 0.5 SM/Chol- $^2\text{H}_5$ plus 0.5 POPC/Chol- $^2\text{H}_5$.

% of cholesterol (10) or egg PC liposomes with 50 mol % (24). In the present study, we do not observe two different powder spectra for cholesterol that could be slowly exchanging (at the μs time scale) between two different environments: the rafts (cholesterol-rich) and the rest of the membrane (cholesterol-poor). This very crucial statement will be further discussed in the next section. We will first consider the dynamics at the nanosecond time scale. Nuclear relaxation times measurements, T_{1Z} and T_{2E} , for cholesterol in the rafts mixtures lead to a single-exponential decay for each of the labeled positions. In addition, the Zeeman relaxation values are quite similar to those reported for the DMPC/Chol- $^2\text{H}_5$ (37) at 35 °C; even though experiments were performed at different Larmor frequencies. This suggests that in all our experiments cholesterol is only in one environment, with a single dynamical behavior.

To further establish whether there are two spectra slowly exchanging at the microsecond time scale, deuterium spectral simulations were performed. Cholesterol deuterium powder spectra of both binary systems POPC/Chol- $^2\text{H}_5$ and SM/Chol- $^2\text{H}_5$ were simulated to match experimental spectra at 30 °C (Figure 5, left part) according to the following procedure: the location of the axis of motional averaging of the cholesterol fused ring moiety was first determined from quadrupolar splittings (vide infra, and Appendix), and then the cholesterol molecular order parameter, S_{mol} , was calculated. S_{mol} was found, respectively, 1.0 and 0.9 for cholesterol in SM and POPC, at 30 °C. These values together with the known C- ^2H bond orientations with respect to the cholesterol symmetry axis were then taken for the spectral simulations. The only variable left was the intrinsic line width of each of the quadrupolar splittings. Figure 5, left, shows the very good agreement between experimental and simulated spectra.

Cholesterol spectra originating from our two "rafts" systems were also submitted to spectral simulations. In the case of SCRL, the spectrum could only be simulated using the same parameters as for the binary SM/Chol- $^2\text{H}_5$ system. This strongly suggests that cholesterol in SCRL systems has

the same properties as in SM, i.e., very ordered. Because the experimental cholesterol spectra of POPC/SM/Chol- $^2\text{H}_5$ have line shapes between those of SM/Chol- $^2\text{H}_5$ and POPC/Chol- $^2\text{H}_5$, we performed simulations using combinations of these two reference spectra, with molecular order parameters of respectively 1.0 and 0.9. Several proportions of both cholesterol environments were added in order to match the experimental spectrum. As seen in Figure 5, right, where combinations of cholesterol environments varied from 9/1 to 1/1, none of them match with the experimental spectrum of raft composition POPC/SM/Chol-d5. Indeed, one can distinguish very different $\Delta\nu_Q$ for the 2,4 equatorial positions if the two simulated references spectra were added in same proportion (bottom spectrum in the right part of Figure 5). In this simulation, the difference between the splittings is 1.7 kHz (2,4 equatorial position). Because the experimental resolution is of a few hundred hertz such a separation could be unequivocally detected on the experimental spectrum. This is not the case (Figure 5, center spectrum). Alternatively, a simulation can be made on the basis of fast exchange between two equally populated pools of cholesterol having individually S_{mol} values of 1 and 0.9. In conclusion, the detection of a unique $\Delta\nu_Q$ on POPC/SM/Chol- $^2\text{H}_5$ raft spectra strongly suggests that cholesterol could be in fast exchange between two or more membrane regions of different dynamics. So the statement of rigid domains made of SM and cholesterol in the model POPC/SM/Chol- $^2\text{H}_5$ raft system is questionable.

Quantitative Determination of Cholesterol Dynamics and Orientation in Rafts. Because of the polycyclic rigid structure of cholesterol, deuterium NMR allows the determination of two structural and dynamical parameters: the location of the principal axis of motion, \bar{n} , and the molecular order parameter, S_{mol} , of cholesterol in the studied mixtures (see theoretical background). The location of \bar{n} in SCRL mixtures at 30 °C is presented in Figure 6 (side and top views in stick and CPK representations, respectively). Not surprisingly the axis of motional averaging lies along the long axis of the molecule and is such that cholesterol offers a minimal cross section of $33 \pm 5 \text{ \AA}^2$, as estimated with the Insight II software. The cholesterol principal axis of motion in rafts and binary systems is found to be the same and independent of temperature. The angles α and β , which define \bar{n} in the molecular frame attached to the molecule as shown in Figure 6, are of 9–12° and 13–15°, respectively. This orientation in the rafts mixtures is identical to that found in a system composed of DMPC/Cholesterol (30% mol) (11). We also calculated the orientation, relative to \bar{n} , of all the carbon-hydrogen bonds attached to the rigid body of cholesterol, Table 1. This table also reports the predicted quadrupolar splitting, for $S_{\text{mol}} = 1$, for each potentially labeled position attached to the polycyclic ring. This table may now be used to directly calculate molecular order parameters from $\Delta\nu_Q$ measurement, without making all the calculations described in the Appendix.

Another interesting result resides in the various values of S_{mol} in relation to membrane composition. The molecular order parameter S_{mol} was calculated as a function of temperature (from 10 to 60 °C) for the four lipids-cholesterol mixtures. Figure 7 depicts a monotonic decrease of S_{mol} when the temperature increases. As a general comment, we observe order parameters greater than 0.8, indicating that, for all

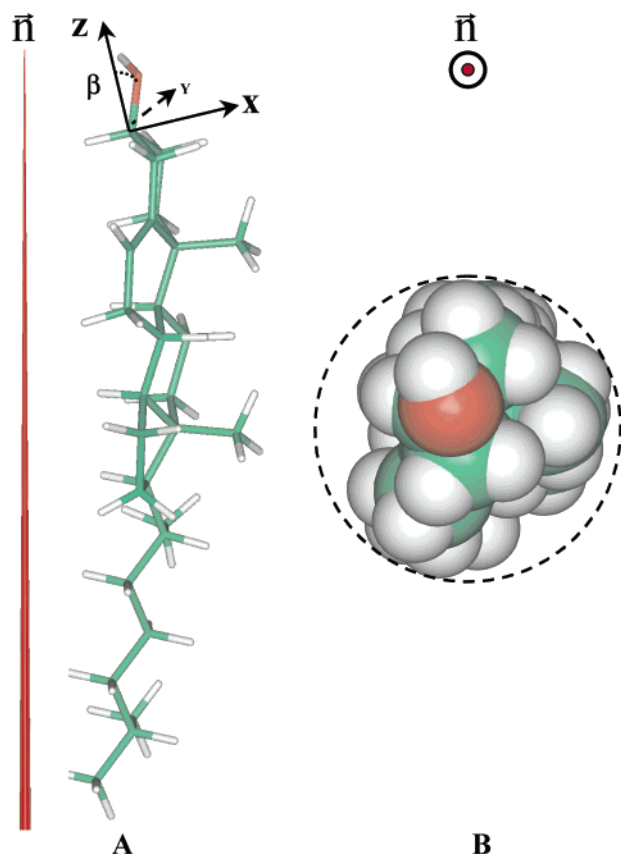


FIGURE 6: (A) Representation (stick mode) of cholesterol average orientation with respect to its principal axis of motional averaging, \vec{n} , when \vec{n} is parallel to the page plane. (B) Same as panel A with \vec{n} , perpendicular to the page plane, CPK representation is used here. The dashed line tentatively represents the cholesterol molecular area when viewed from above the membrane surface. The x,y,z axes of the cholesterol-attached frame of reference (see Appendix) are also shown in panel A. The angle β is that between \vec{n} and z .

systems, the cone semiangle for cholesterol wobbling is less than 13° , even at 60°C . The binary mixtures present “boundary” profiles with the lowest values for POPC/Chol- $^2\text{H}_5$ system and the highest for SM/Chol- $^2\text{H}_5$. The thermal behavior of S_{mol} in the two raft compositions is quite different. The SCRL raft mixture has the same S_{mol} variation as the SM/Chol- $^2\text{H}_5$, i.e., the highest S_{mol} values over the temperature range. It means that in the SCRL mixtures, in which domains have been already put forward on the basis of ultra centrifugation analyses (25), cholesterol has the same dynamics (almost no oscillations) as in the binary system SM/Chol. Of course the complex SCRL mixture has nothing to do with the model membrane made of SM and Chol. But our finding strongly suggests that cholesterol is depleted from the rest of the membrane to form complexes of same dynamics as if it was alone with SM. On the other hand, the mixture POPC/SM/Chol- $^2\text{H}_5$ exhibits an intermediate S_{mol} profile between those of SM/Chol and POPC/Chol. This strongly suggests that cholesterol could be in fast exchange between two or more membrane regions of different dynamics. So the statement of rigid domains made of SM and cholesterol in the model raft system POPC/SM/Chol- $^2\text{H}_5$ is questionable. In this case, rafts were proposed on the basis of fluorescence experiments using Laurdan (7). The argument of techniques operating at different time scales cannot be put forward because of our nuclear relaxation experiments

Table 1: Carbon–Deuterium Bond Orientations and Corresponding Quadrupolar Splittings of Cholesterol in Biomembranes

| carbon position | deuteron position | γ_i (deg) ^a | $\Delta\nu_Q(90^\circ)$ (kHz) ^b |
|-----------------|-------------------|-------------------------------|--|
| C1 | ax | 102.8 | 53.4 |
| | eq. | 113.0 | 33.9 |
| C2 | ax | 74.7 | 49.5 |
| | eq. | 67.7 | 35.6 |
| C3 | ax | 102.8 | 53.4 |
| C4 | ax | 67.7 | 35.6 |
| | eq. | 72.2 | 45.1 |
| C6 | | 56.3 | 4.8 |
| C7 | ax | 106.9 | 46.7 |
| | eq. | 105.0 | 50.0 |
| C8 | ax | 88.4 | 62.5 |
| C9 | ax | 89.8 | 62.6 |
| C11 | ax | 87.4 | 62.2 |
| | eq. | 66.1 | 31.8 |
| C12 | ax | 117.8 | 21.8 |
| | eq. | 94.2 | 61.6 |
| C14 | ax | 87.8 | 62.3 |
| C15 | ax | 77.6 | 54.0 |
| | eq. | 81.5 | 58.5 |
| C16 | ax | 117.1 | 23.6 |
| | eq. | 123.7 | 4.8 |

^a Angle between the i th C- ^2H bond and the axis of motional averaging of cholesterol. ^b Predicted quadrupolar splitting [$\Delta\nu_Q(90^\circ)$] with a S_{mol} value of 1 (using eqs 1 and 2 of text). Estimated accuracy of 5%.

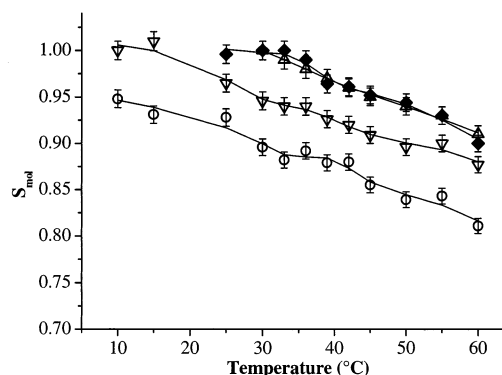


FIGURE 7: Thermal variation of the cholesterol molecular order parameter S_{mol} in the four lipid-cholesterol compositions. (○) POPC/Chol- $^2\text{H}_5$, (△) SM/Chol- $^2\text{H}_5$, (▽) POPC/SM/Chol- $^2\text{H}_5$, (◆) SCRL/Chol- $^2\text{H}_5$. Accuracy is 2%.

on cholesterol. They report on dynamical events occurring at the nanosecond, as in fluorescence measurements. Recent work on the ternary system POPE/SM/Chol also concluded that POPE lipid did not separate from the rest of the membrane (38). Although POPC and POPE differ by their headgroup, this result is in complete accordance with ours.

CONCLUSION

Solid-state NMR was used to investigate the controversial hypothesis of lipids microdomains in model membranes. This nonperturbing approach afforded to detect the liquid-ordered phase (Lo) in fully hydrated systems of “raft” composition at physiological temperatures. Using deuterium-labeled cholesterol as a direct reporter, its ordering properties and orientation in putative domains were determined. The cholesterol moiety is almost parallel to the normal to the bilayer in all systems investigated. The dynamics of cholesterol as defined by its molecular order parameter is very high in all systems. It is the same in the SCRL mixture as in the simple SM/Chol system, which favors the existence of

highly rigid SM/Chol domains. Cholesterol ordering in the POPC/SM/Chol "raft" mixture is between those of POPC/Chol and SM/Chol binary systems, a situation that is not in favor of domain formation.

APPENDIX

The method to find both the location of the axis of motional averaging and the molecular order parameter is derived from that of Taylor (24) and Dufourc (10). It is outlined here for clarity. The atomic coordinates of the cholesterol structure have been extracted from neutron diffraction experiments (39). In a first step, a coordinate system, C, is attached to the C₃ carbon atom of cholesterol and is defined such that the *x*-axis is collinear with the C₃–H axial bond and the *z*-axis belongs to the –O–C₃–H plane (left part of Figure 6). The original crystal coordinates have been transformed into the C system by one translation and three successive rotations. The axis of motion \vec{n} (aligned along the bilayer normal) is defined in the axis system C as $\vec{n} = (\cos\alpha \sin\beta, \sin\alpha \sin\beta, \cos\beta)$. The angle γ_i that an individual C–²H_i bond vector makes with the axis of motion can be defined as

$$\cos \gamma_i = \frac{l_i \cos \alpha \sin \beta + m_i \sin \alpha \sin \beta + n_i \cos \beta}{\|\vec{C} - \vec{i}\| \cdot \|\vec{n}\|}$$

where l_i , m_i , and n_i are the direction cosines of the C–²H_i bond vector obtained from the atomic coordinates of carbon and deuterium atoms in the C axis system. Because the direction cosines of each C–²H bond are known, one may automatically vary the α and β angles to compute $(3 \cos^2 \gamma_i - 1)/2$ terms and evaluate the ratio $R_{i,j}^C = (3 \cos^2 \gamma_i - 1)/(3 \cos^2 \gamma_j - 1)$. The latter can be compared to its experimental counterpart, $R_{i,j}^E = \Delta\nu_Q^i(90^\circ)/\Delta\nu_Q^j(90^\circ)$, obtained from the ratio of quadrupolar splittings relative to C–²H_i and C–²H_j bonds. This method of calculation is based upon the hypothesis of rigidity of the sterol fused ring structure (same S_{mol} value for all of its C–²H bonds). The geometrical position of the cholesterol motional axis is then determined by varying the angles α and β . An automated algorithm (FORTRAN routine, E.J.D. and F.A., unpublished material) searches for the minimum deviation $D = \sum_i [(R_{i,j}^C - R_{i,j}^E)/R_{i,j}^E]^2$ (<0.02): the position of the principal of motion for the rigid moiety is then determined by a particular set of angles α and β . Once the correct orientation of \vec{n} has been defined relative to C, the term $(3 \cos^2 \gamma_i - 1)/2$ is known for a given C–²H_i bond and S_{mol} can thus be obtained from eq 2 (see Theoretical Background). Because five S^{CD} s are known, an average is made.

REFERENCES

1. Simons, K., and Ikonen, E. (1997) *Nature* 387, 569–572.
2. London, E., and Brown, D. A. (2000) *Biochim. Biophys. Acta* 1508, 182–195.
3. Verkade, P., and Simons, K. (1997) *Histochem. Cell. Biol.* 108, 211–220.
4. Jacobson, K., and Dietrich, C. (1999) *Tr. Cell Biol.* 9, 87–91.
5. Samsonov, A., Mihalyov, I., and Cohen, F. S. (2001) *Biophys. J.* 81, 1486–1500.
6. Ahmed, S. N., Brown, D. A., and London, E. (1997) *Biochemistry* 36, 10944–10953.
7. Dietrich, C., Bagatolli, L. A., Volovyk, Z. N., Thompson, N. L., Levi, M., Jacobson, K., and Gratton, E. (2001) *Biophys. J.* 80, 1417–1428.
8. Yuan, C., Furlong, J., Burgos, P., and Johnston, L. J. (2002) *Biophys. J.* 82, 2526–2535.
9. Oldfield, E., Meadows, M., Rice, D., and Jacobs, R. (1978) *Biochemistry* 17, 2727–1739.
10. Dufourc, E. J., Parish, E. J., Chitrakorn, S., and Smith, I. C. P. (1984) *Biochemistry* 23, 6063–6071.
11. Marsan, M. P., Muller, I., Ramos, C., Rodriguez, F., Dufourc, E. J., Czaplicki, J., and Milon, A. (1999) *Biophys. J.* 76, 351–359.
12. Douliez, J. P., Léonard, A., and Dufourc, E. J. (1996) *J. Phys. Chem.* 100, 18450–18457.
13. Seelig, A., and Seelig, J. (1977) *Biochemistry* 16, 45–50.
14. Ipsen, J. H., Karlström, G., Mouritsen, O. G., Wennerström, H., and Zuckermann, M. J. (1987) *Biochim. Biophys. Acta* 905, 162–172.
15. Ipsen, J. H., Mouritsen, O. G., and Bloom, M. (1990) *Biophys. J.* 52, 405–412.
16. Vist, M. R., and Davis, J. H. (1990) *Biochemistry* 29, 451–464.
17. Davis, J. H. (1983) *Biochim. Biophys. Acta* 737, 117–171.
18. Seelig, J. (1978) *Biochimica Biophysica Acta* 515, 105–140.
19. Marinov, R., and Dufourc, E. J. (1995) *J. Chim. Phys.* 92, 1727–1731.
20. Killian, J. A., Verkleij, A. J., Leunissen-Bijeveld, J., and De Kruijff, B. (1985) *Biochim. Biophys. Acta* 812, 21–26.
21. Franzin, C. M., and Macdonald, P. M. (2001) *Biophys. J.* 81, 3346–3362.
22. Douliez, J. P., Léonard, A., and Dufourc, E. J. (1995) *Biophys. J.* 68, 1727–1739.
23. Helfrich, W. (1973) *Z. Naturforsch.* 28, 693–703.
24. Taylor, M. G., Akiyama, T., and Smith, I. C. P. (1981) *Chem. Phys. Lipids* 29, 327–339.
25. Schroeder, R., London, E., and Brown, D. (1994) *Proc. Natl. Acad. Sci. U.S.A.* 91, 12130–12134.
26. Rance, M., and Byrd, R. A. (1983) *J. Magn. Reson.* 52, 221–240.
27. Davis, J. H., Jeffrey, K. R., Bloom, M., Valic, M. I., and Higgs, T. P. (1976) *Chem. Phys. Lett.* 42, 390–394.
28. Bloom, M., Davis, J. H., and Mackay, A. L. (1981) *Chem. Phys. Lett.* 80, 198–201.
29. Sternin, E., Bloom, M., and MacKay, A. L. (1983) *J. Magn. Reson.* 55, 274–282.
30. Seelig, J. (1977) *Q. Rev. Biophys.* 10, 353–418.
31. Burnett, L. J., and Müller, B. H. (1971) *J. Chem. Phys.* 55, 5829–5831.
32. Petersen, N. O., and Chan, S. I. (1977) *Biochemistry* 16, 2657–2667.
33. Dufourc, E. J., Mayer, C., Stohrer, J., Althoff, G., and Kothe, G. (1992) *Biophys. J.* 61, 42–57.
34. Pott, T., Paternostre, M., and Dufourc, E. J. (1998) *Eur. Biophys. J.* 27, 237–245.
35. Guo, W., Kurze, V., Huber, T., Nezan, H. A., Beyer, K., and Hamilton, J. A. (2002) *Biophys. J.* 83, 1465–1478.
36. Brzustowicz, M. R., Cherezov, V., Caffrey, M., Stillwell, W., and Wassall, S. R. (2002) *Biophys. J.* 82, 285–298.
37. Dufourc, E. J., and Smith, I. C. P. (1986) *Chem. Phys. Lipids* 41, 123–135.
38. Shaikh, S. R., Brzustowicz, M. R., Gustafson, N., Stillwell, W., and Wassall, S. R. (2002) *Biochemistry* 41, 10593–10602.
39. McMullan, R. K., Koetzle, T. F., and Fronckowiak, M. D. (1992) *Acta Crystallogr.* 48, 1509–1512.

BI026717B